**Supplementary Materials**

# New Quinazolin-4(3*H*)-one Derivatives Incorporating Hydrazone and Pyrazole Scaffolds as Antimicrobial Agents Targeting DNA Gyraze Enzyme

**Eman M. Mohi El-Deen [1,*], Eman S. Nossier [2], Eman A. Karam [3]**

[1] Department of Therapeutic Chemistry, National Research Centre, Dokki, Cairo, 12622 Egypt
[2] Department of Pharmaceutical Medicinal Chemistry, Faculty of Pharmacy (Girls), Al-Azhar University, Cairo 11754, Egypt
[3] Microbial Chemistry Department, National Research Centre, Dokki, Cairo, 12622 Egypt
* Correspondence: e.mohi.2010@live.com; Tel.: +20-0106-385-3338.

## Table of contents

| Subject | Page |
|---|---|
| Figure S1. $^{1}$H-NMR (500 MHz, DMSO-$d_6$) spectrum of **2**. | 3 |
| Figure S2. $^{13}$C-NMR (125 MHz, DMSO- $d_6$) spectrum of **2**. | 3 |
| Figure S3. I.R spectrum of **2**. | 4 |
| Figure S4. Mass spectrum of **2**. | 4 |
| Figure S5. $^{1}$H-NMR (500 MHz, DMSO-$d_6$) spectrum of **4a**. | 5 |
| Figure S6. $^{13}$C-NMR (125 MHz, DMSO- $d_6$) spectrum of **4a**. | 5 |
| Figure S7. I.R spectrum of **4a**. | 6 |
| Figure S8. Mass spectrum of **4a**. | 6 |
| Figure S9. $^{1}$H-NMR (500 MHz, DMSO-$d_6$) spectrum of **4b**. | 7 |
| Figure S10. $^{13}$C-NMR (125 MHz, DMSO- $d_6$) spectrum of **4b**. | 7 |
| Figure S11. I.R spectrum of **4b**. | 8 |
| Figure S12. Mass spectrum of **4b**. | 8 |
| Figure S13. $^{1}$H-NMR (500 MHz, DMSO- $d_6$) spectrum of **4c**. | 9 |
| Figure S14. $^{13}$C-NMR (125 MHz, DMSO- $d_6$) spectrum of **4c**. | 9 |
| Figure S15. $^{1}$H-NMR (500 MHz, DMSO- $d_6$) spectrum of **4d**. | 10 |
| Figure S16. $^{13}$C-NMR (125 MHz, DMSO- $d_6$) spectrum of **4d.** | 10 |
| Figure S17. $^{1}$H-NMR (500 MHz, DMSO- $d_6$) spectrum of **4e**. | 11 |
| Figure S18. $^{13}$C-NMR (125 MHz, DMSO- $d_6$) spectrum of **4e**. | 11 |
| Figure S19. I.R spectrum of **4e.** | 12 |
| Figure S20. $^{1}$H-NMR (500 MHz, DMSO- $d_6$) spectrum of **4f**. | 12 |
| Figure S21. $^{13}$C-NMR (125 MHz, DMSO- $d_6$) spectrum of **4f**. | 13 |
| Figure S22. I.R spectrum of **4f.** | 13 |
| Figure S23. $^{1}$H-NMR (500 MHz, DMSO- $d_6$) spectrum of **5a**. | 14 |
| Figure S24. $^{13}$C-NMR (125 MHz, DMSO- $d_6$) spectrum of **5a**. | 14 |
| Figure S25. I.R spectrum of **5a.** | 15 |
| Figure S26. $^{1}$H-NMR (500 MHz, DMSO- $d_6$) spectrum of **5b**. | 15 |
| Figure S27. $^{13}$C-NMR (125 MHz, DMSO- $d_6$) spectrum of **5b.** | 16 |

| Subject | Page |
| --- | --- |
| Figure S28. $^{1}$H-NMR (500 MHz, DMSO- $d_6$) spectrum of **5c.** | 16 |
| Figure S29. $^{13}$C-NMR (125 MHz, DMSO- $d_6$) spectrum of **5c.** | 17 |
| Figure S30. $^{1}$H-NMR (500 MHz, DMSO- $d_6$) spectrum of **5d.** | 17 |
| Figure S31. $^{13}$C-NMR (125 MHz, DMSO- $d_6$) spectrum of **5d**. | 18 |
| Figure S32. The 3D binding poses of **4a, 5a, 5c** and **5d** within the active site of *E. coli* DNA gyrase. | 19, 20 |
| S33. Minimum Inhibitory Concentration (MIC) Measurement. | 21 |
| S34. *Escherichia coli* DNA Gyrase Supercoiling Inhibition Assay | 22 |
| S35. Molecular docking determination | 23 |

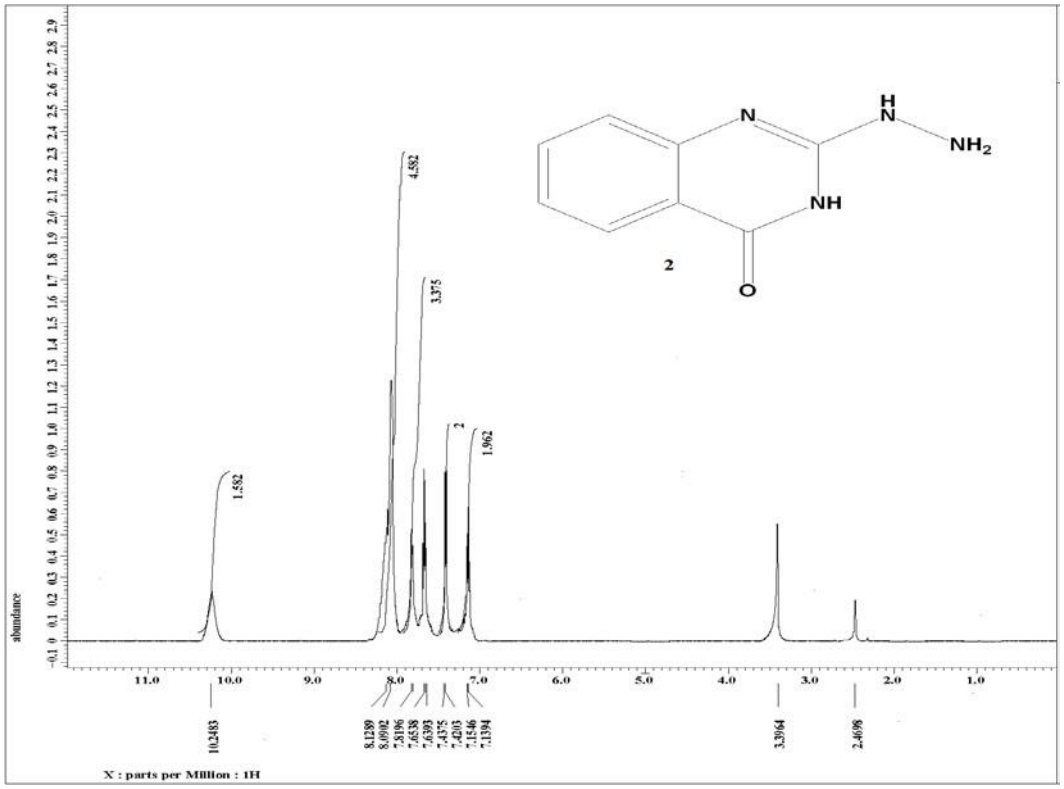


**Fig. S1** $^{1}$H NMR (500 MHz) in DMSO-$d_6$ of compound **2**

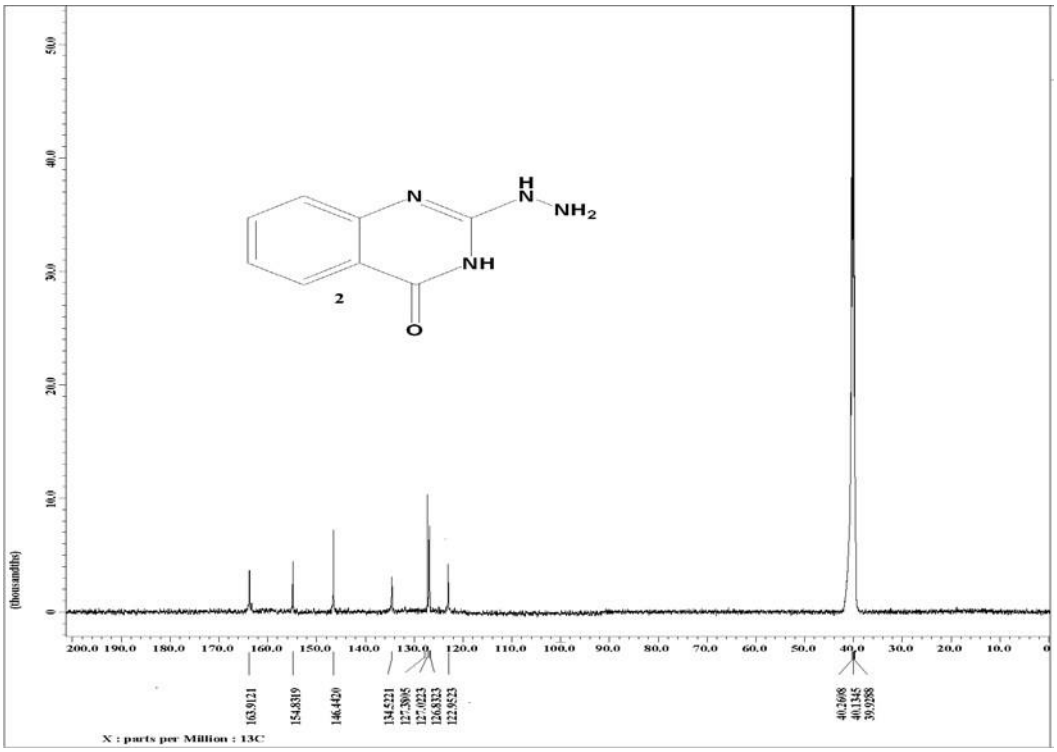


**Fig. S2** $^{13}$C NMR (125 MHz) in DMSO-$d_6$ of compound **2**

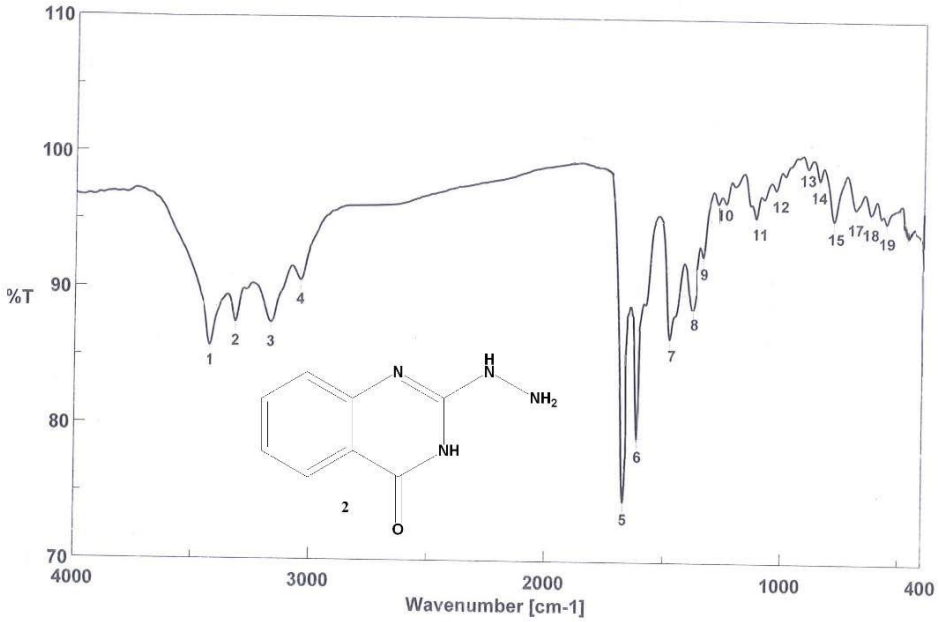


| No. | cm-1 | %T | No. | cm-1 | %T | No. | cm-1 | %T |
|---|---|---|---|---|---|---|---|---|
| 1 | 3431.6 | 85.5908 | 2 | 3308.93 | 87.4848 | 3 | 3187.47 | 87.4409 |
| 4 | 3036.12 | 90.5621 | 5 | 1674.8 | 74.2326 | 6 | 1601.8 | 78.7326 |
| 7 | 1479.13 | 86.5071 | 8 | 1381.75 | 88.7179 | 9 | 1341.25 | 92.5819 |
| 10 | 1279.54 | 96.5032 | 11 | 1118.51 | 95.502 | 12 | 1033.66 | 97.5862 |
| 13 | 895.773 | 99.2028 | 14 | 848.525 | 98.3168 | 15 | 783.922 | 95.3537 |
| 16 | 691.355 | 96.2078 | 17 | 626.752 | 95.8612 | 18 | 556.363 | 95.2081 |
| 19 | 426.752 | 96.5215 | | | | | | |

**Fig. S3** I.R spectrum of compound **2**

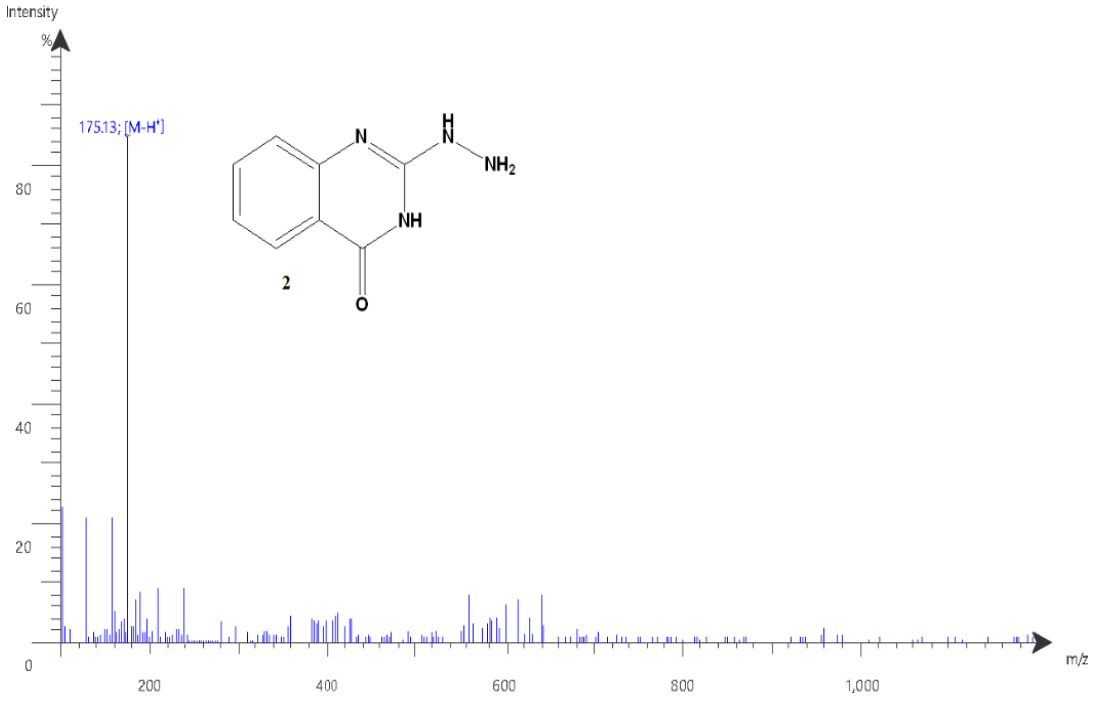


**Fig. S4** ESI-MS spectrum of compound **2**

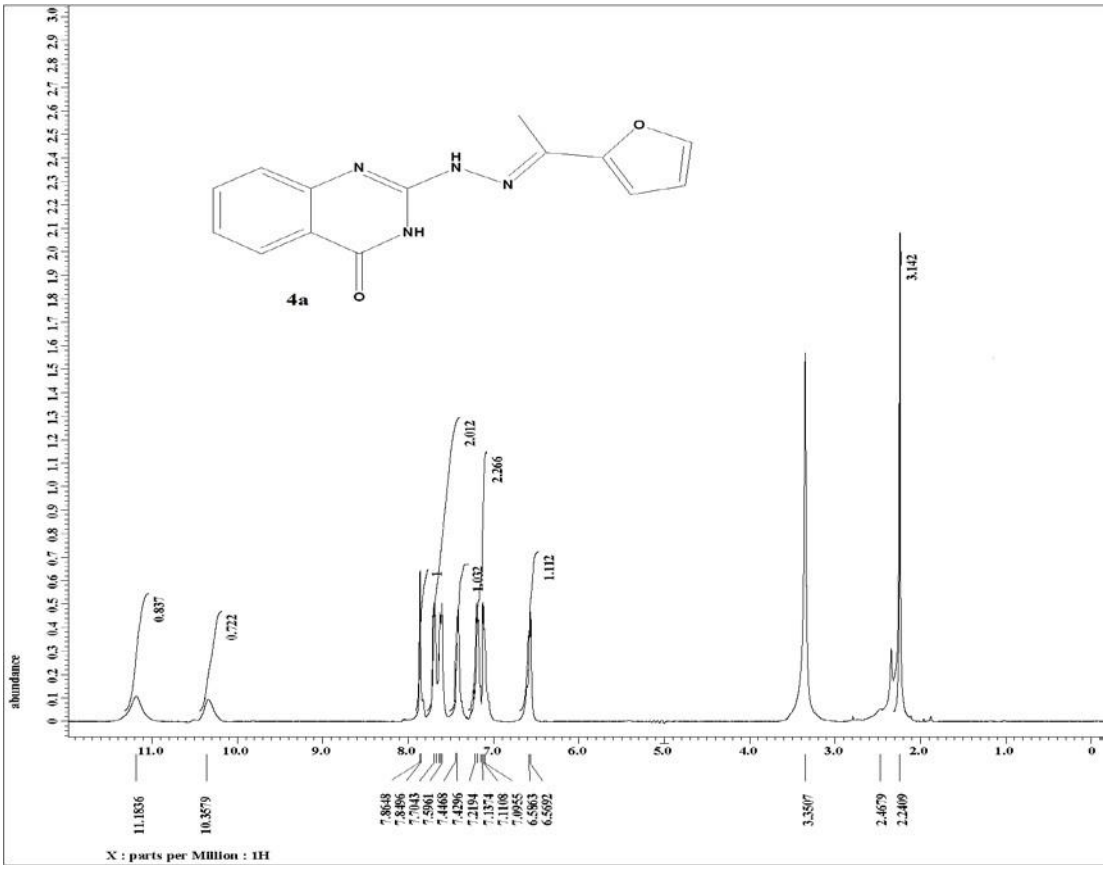


**Fig. S5** $^{1}$H NMR (500 MHz) in DMSO-$d_6$ of compound **4a**

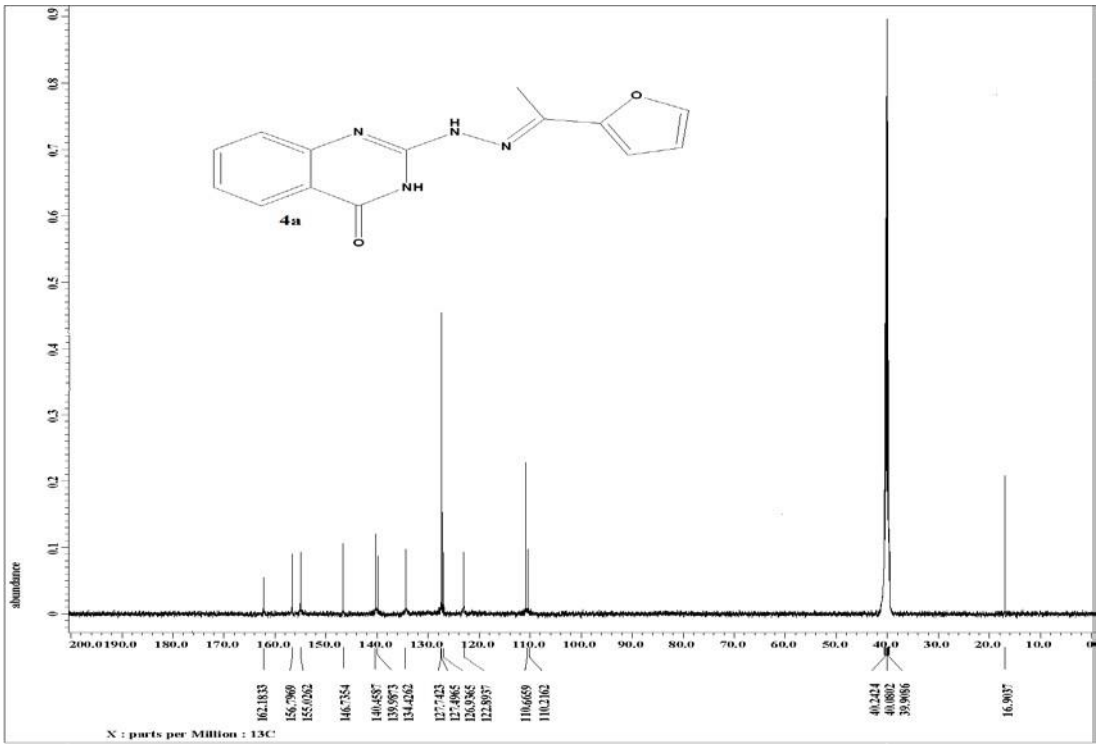


**Fig. S6** $^{13}$C NMR (125 MHz) in DMSO-$d_6$ of compound **4a**

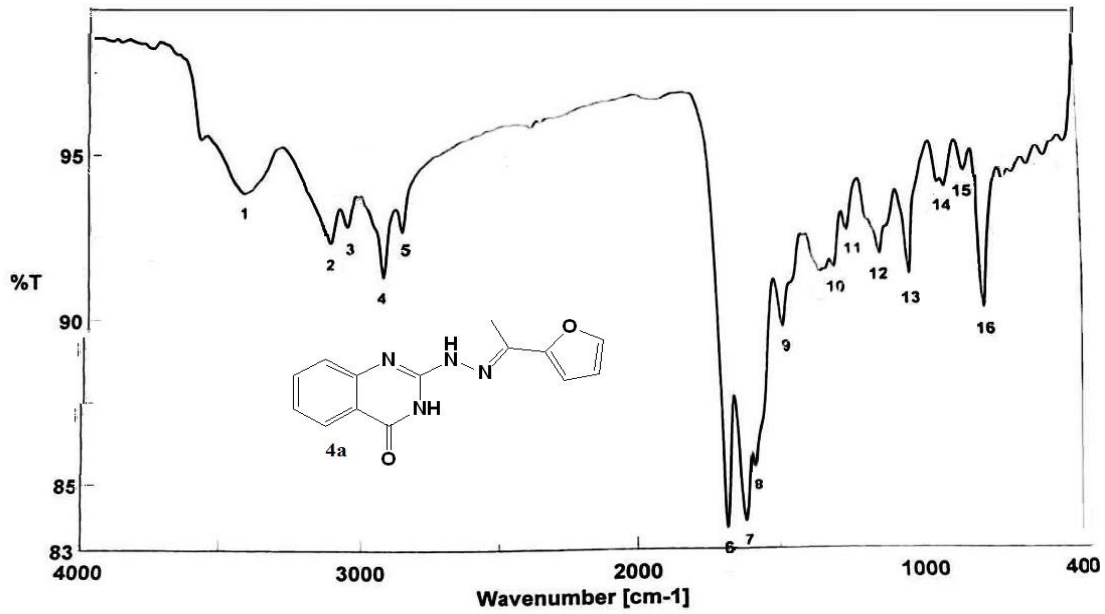


| No. | cm-1 | %T | No. | cm-1 | %T | No. | cm-1 | %T |
|---|---|---|---|---|---|---|---|---|
| 1 | 3420.81 | 93.8484 | 2 | 3114.47 | 92.2022 | 3 | 3041.47 | 92.7622 |
| 4 | 2919.7 | 91.1704 | 5 | 2851.24 | 92.5611 | 6 | 1683.55 | 83.603 |
| 7 | 1618.95 | 83.8055 | 8 | 1579.15 | 85.4546 | 9 | 1476.24 | 89.5995 |
| 10 | 1335.46 | 91.2734 | 11 | 1236.15 | 92.5546 | 12 | 1121.4 | 91.7963 |
| 13 | 1016.3 | 91.1723 | 14 | 883.238 | 93.8151 | 15 | 810.92 | 94.2847 |
| 16 | 752.102 | 90.1462 | | | | | | |

**Fig. S7** I.R spectrum of compound **4a**

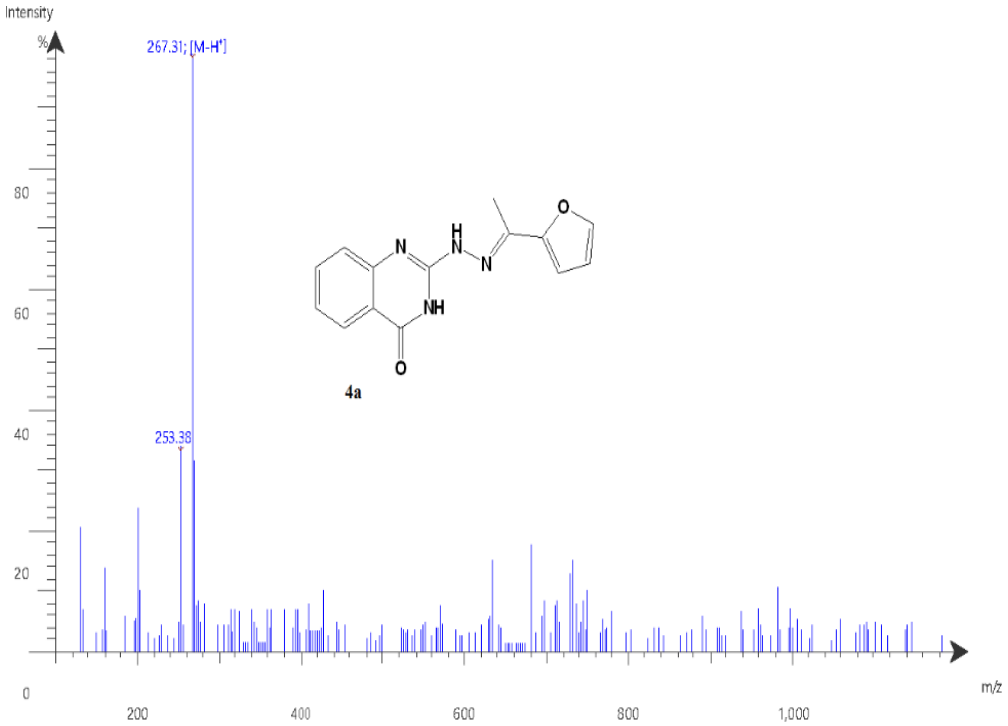


**Fig. S8** ESI-MS spectrum of compound **4a**

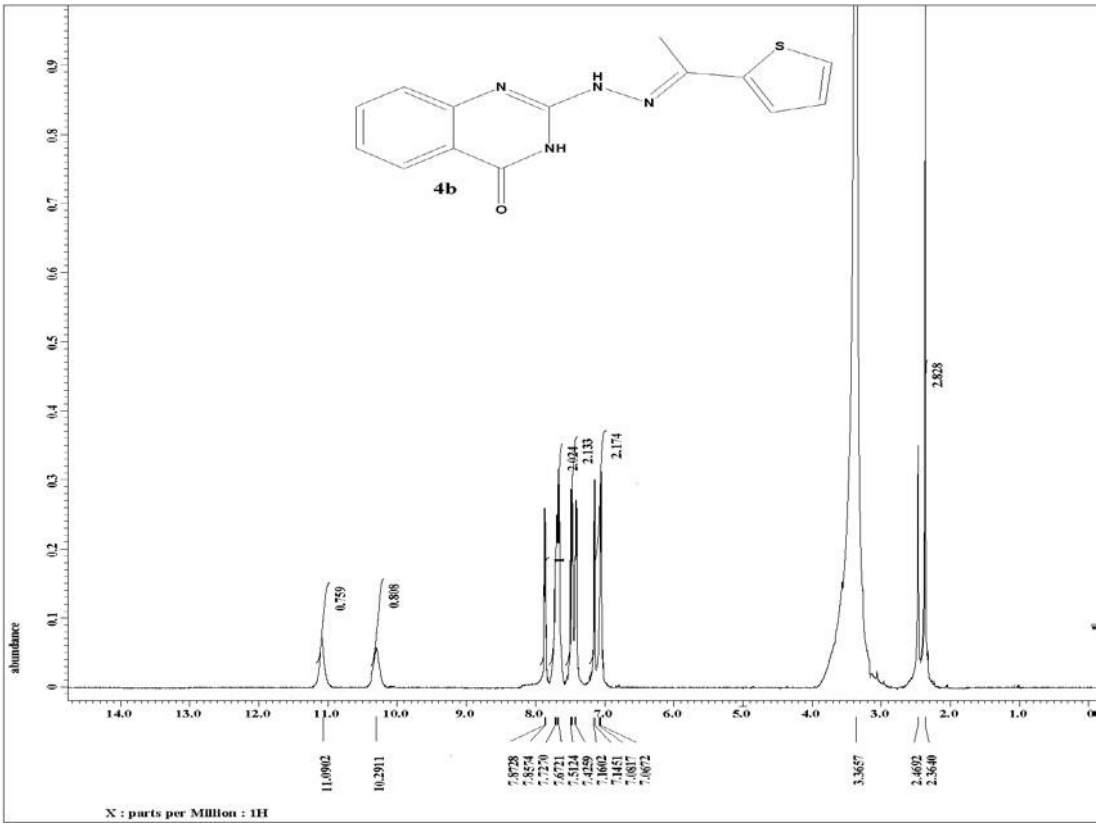


**Fig. S9** $^{1}$H NMR (500 MHz) in DMSO-$d_6$ of compound **4b**

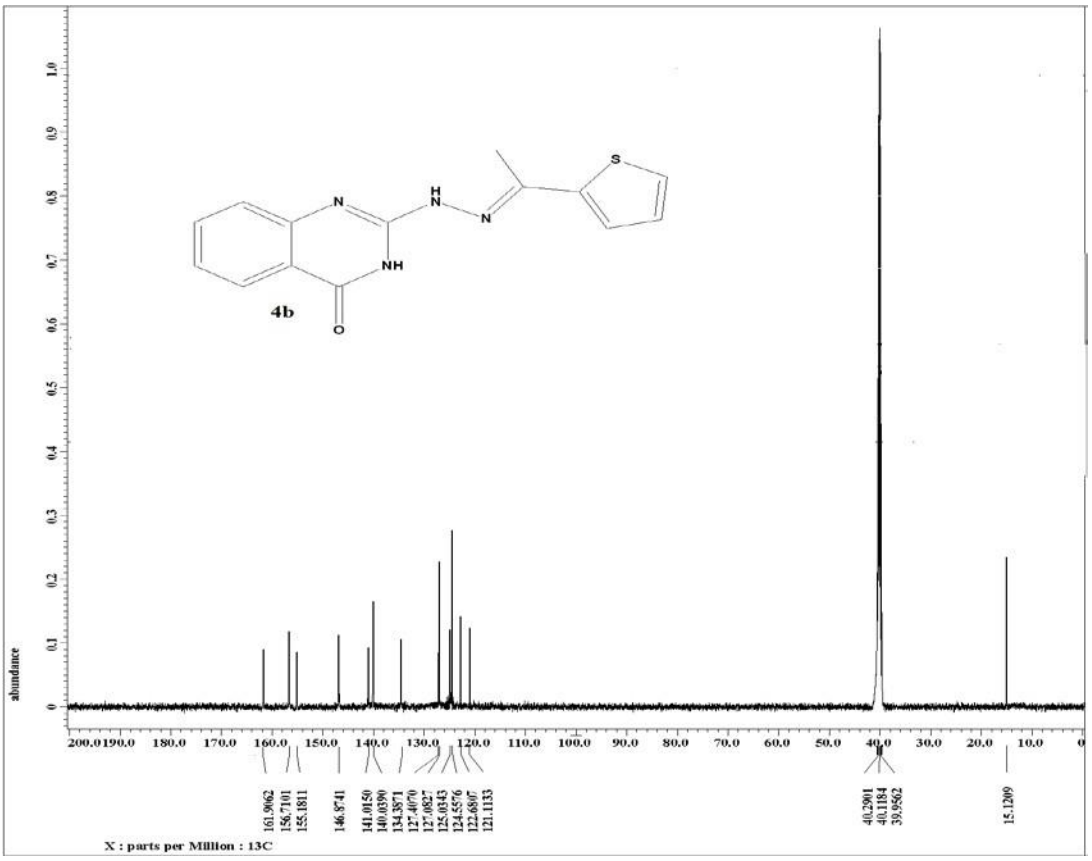

**Fig. S10** $^{1}$H NMR (500 MHz) in DMSO-$d_6$ of compound **4b**

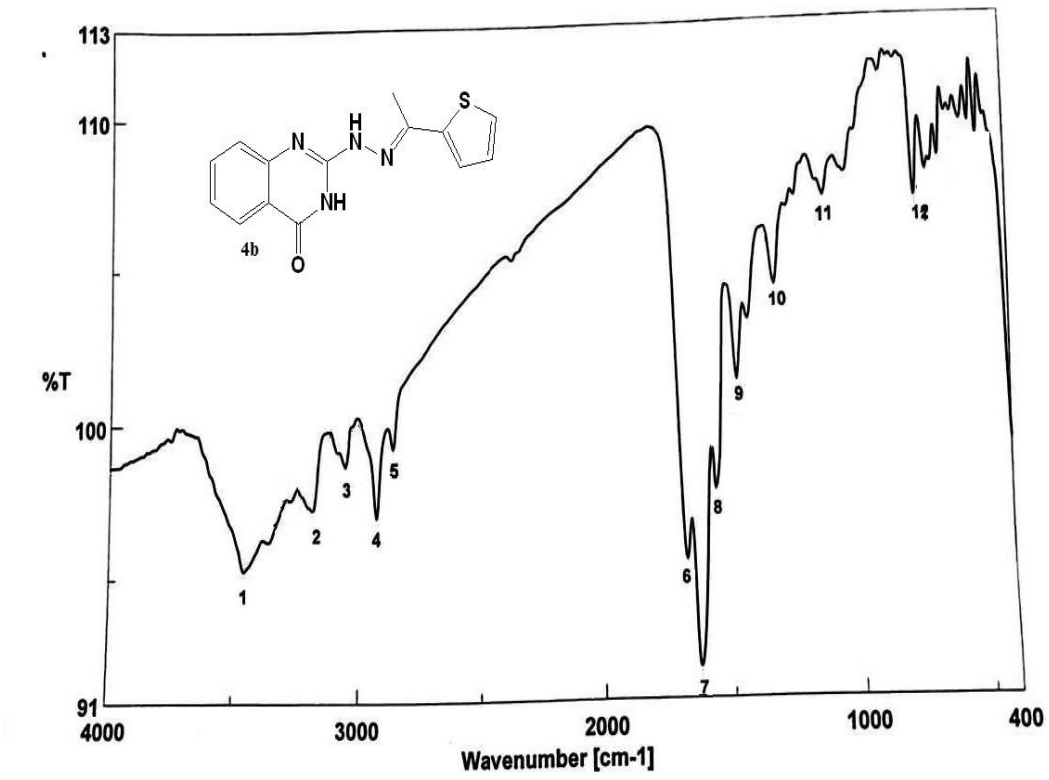


| No. | cm-1 | %T | No. | cm-1 | %T | No. | cm-1 | %T |
|---|---|---|---|---|---|---|---|---|
| 1 | 3452.92 | 95.2263 | 2 | 3164.92 | 96.5206 | 3 | 3044.96 | 97.5263 |
| 4 | 2919.7 | 96.2825 | 5 | 2858.2 | 99.071 | 6 | 1680.66 | 95.3383 |
| 7 | 1630.52 | 91.995 | 8 | 1582.28 | 96.0625 | 9 | 1475.28 | 101.088 |
| 10 | 1320.04 | 104.189 | 11 | 1120.44 | 107.045 | 12 | 757.888 | 106.93 |

**Fig. S11** I.R spectrum of compound **4b**

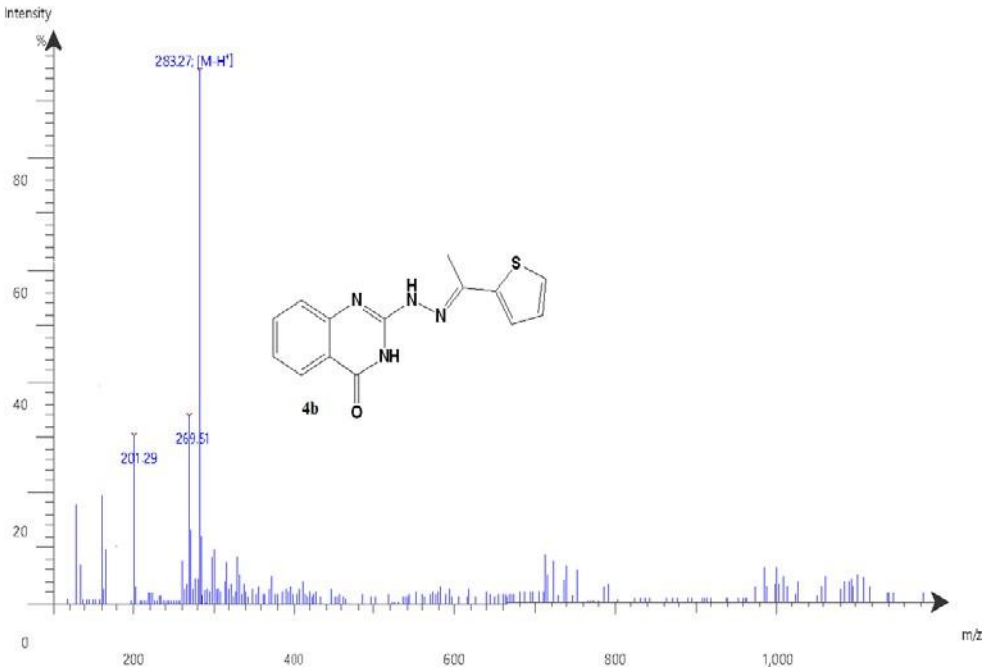

**Fig. S12** ESI-MS spectrum of compound **4b**

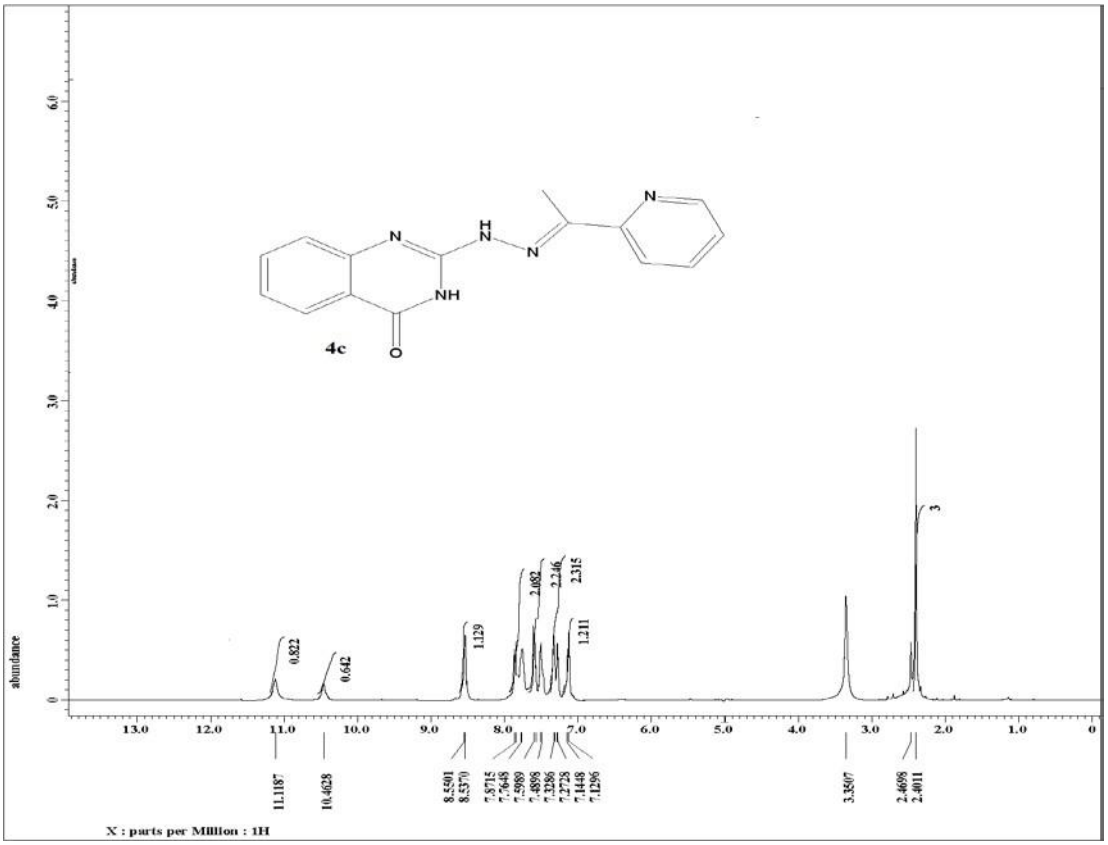


**Fig. S13** $^{1}$H NMR (500 MHz) in DMSO-$d_6$ of compound **4c**

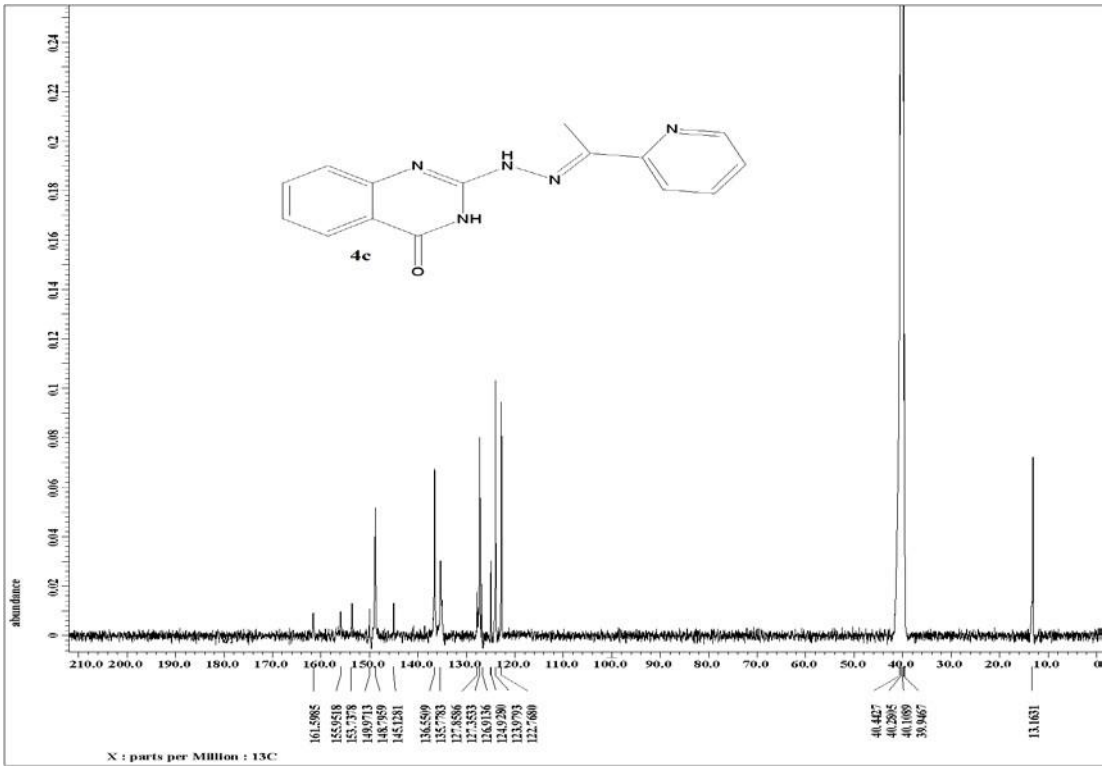


**Fig. S14** $^{13}$C NMR (125 MHz) in DMSO-$d_6$ of compound **4c**

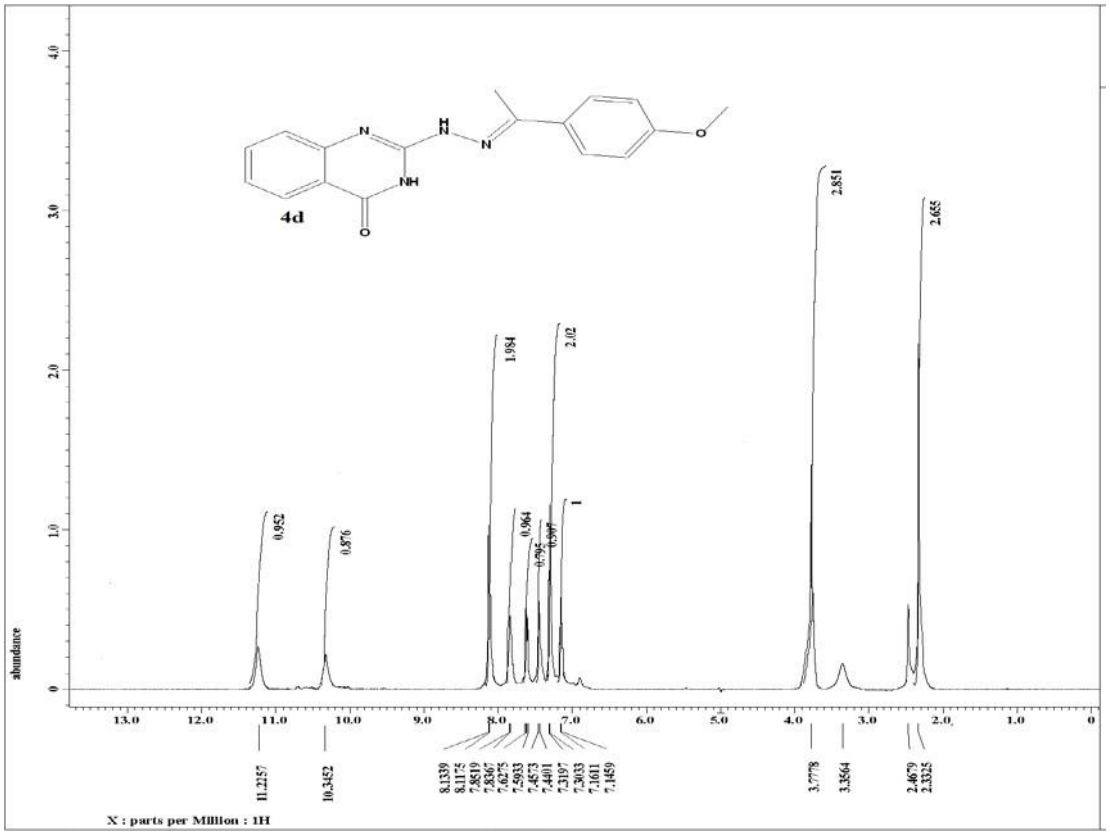


**Fig. S15** $^{1}$H NMR (500 MHz) in DMSO-$d_6$ of compound **4d**

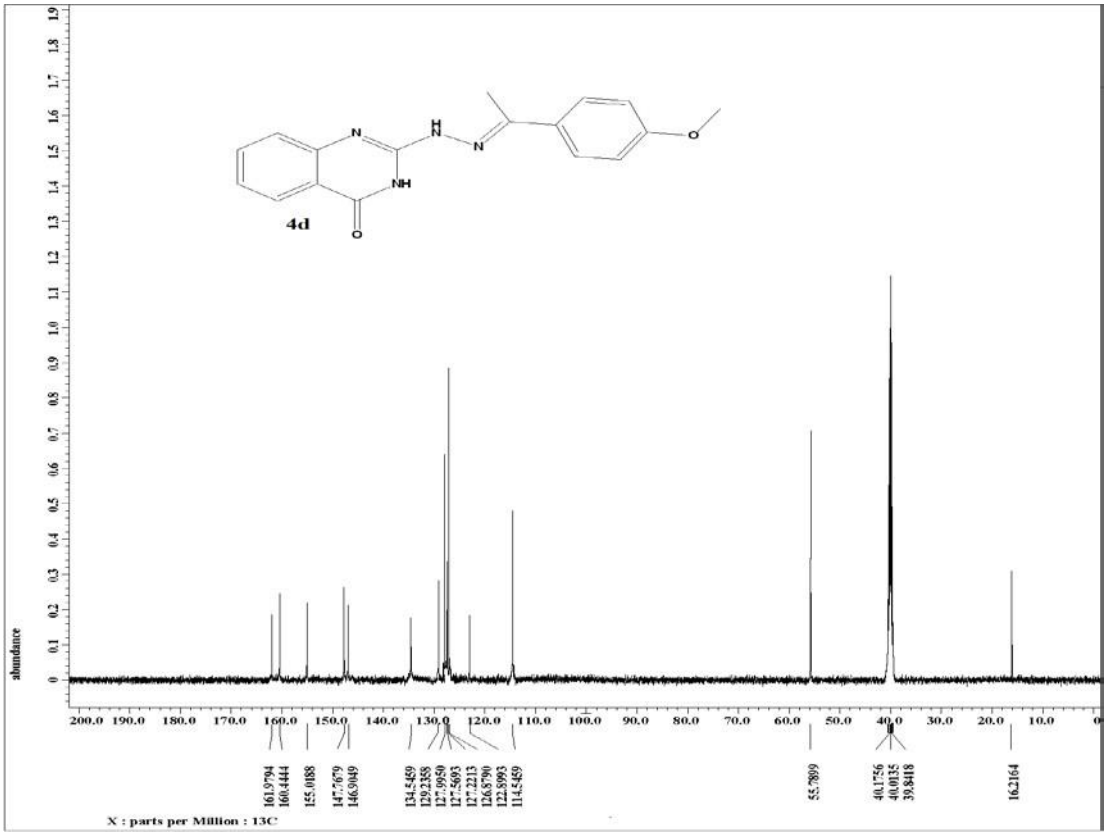

**Fig. S16** $^{13}C$ NMR (125 MHz) in DMSO-$d_6$ of compound **4d**

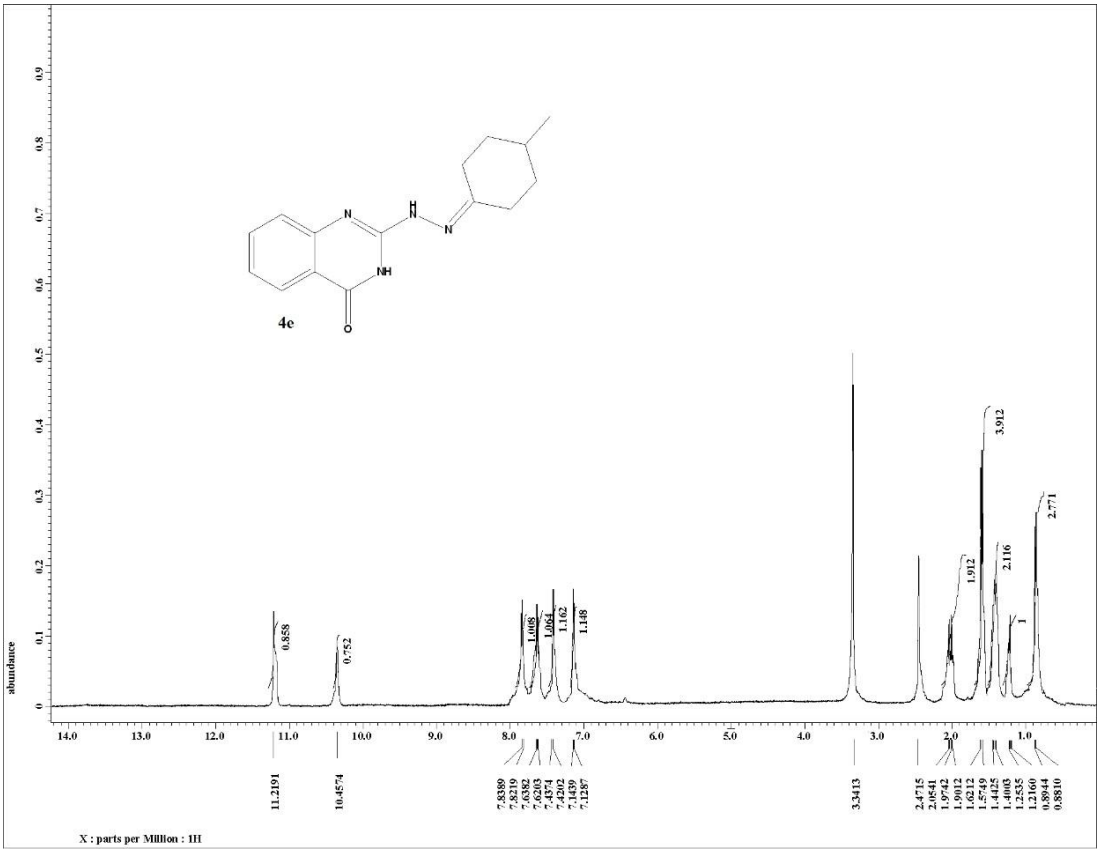


**Fig. S17** $^{1}$H NMR (500 MHz) in DMSO-$d_6$ of compound **4e**

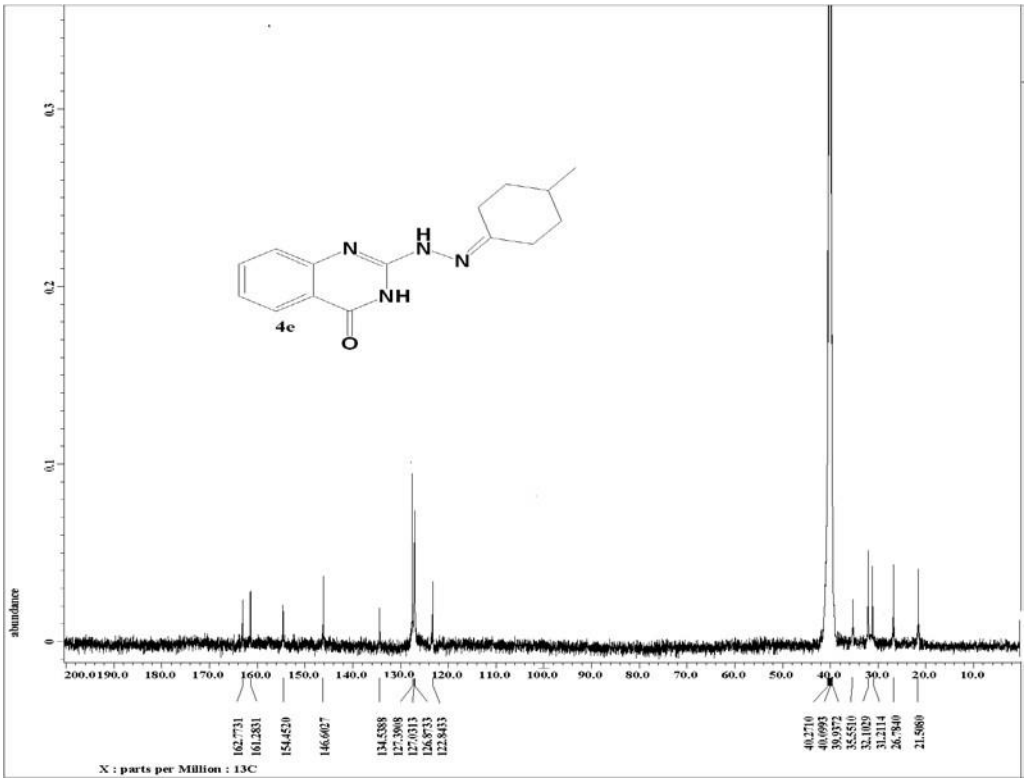

**Fig. S18** $^{13}C$ NMR (125 MHz) in DMSO-$d_6$ of compound **4e**

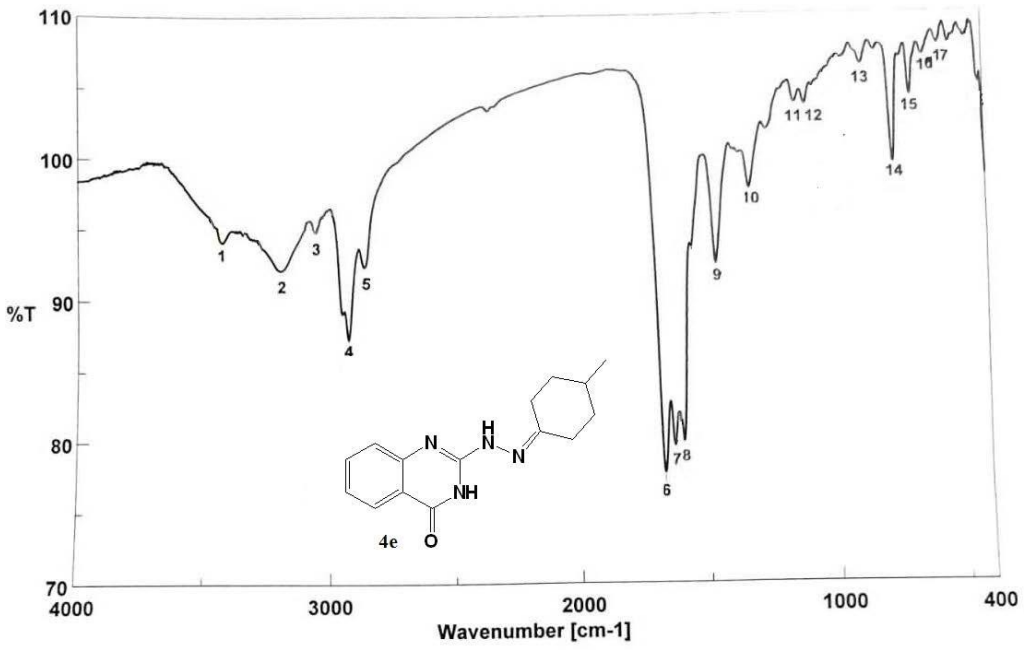


| | cm-1 | %T | No. | cm-1 | %T | No. | cm-1 | %T |
|---|---|---|---|---|---|---|---|---|
| | 3422.48 | 94.9516 | 2 | 3192.58 | 91.9411 | 3 | 3036.54 | 94.8711 |
| | 2923.56 | 86.9973 | 5 | 2861.84 | 92.1136 | 6 | 1676.8 | 77.5677 |
| | 1638.23 | 79.4267 | 8 | 1598.23 | 79.7155 | 9 | 1470.46 | 92.1535 |
| 0 | 1334.5 | 97.5113 | 11 | 1148.4 | 103.584 | 12 | 1108.87 | 103.466 |
| 3 | 884.202 | 106.258 | 14 | 762.709 | 99.2078 | 15 | 690.391 | 104.042 |
| 5 | 635.43 | 106.903 | 17 | 576.612 | 107.66 | 18 | 533.221 | 107.681 |

**Fig. S19** I.R spectrum of compound **4e**

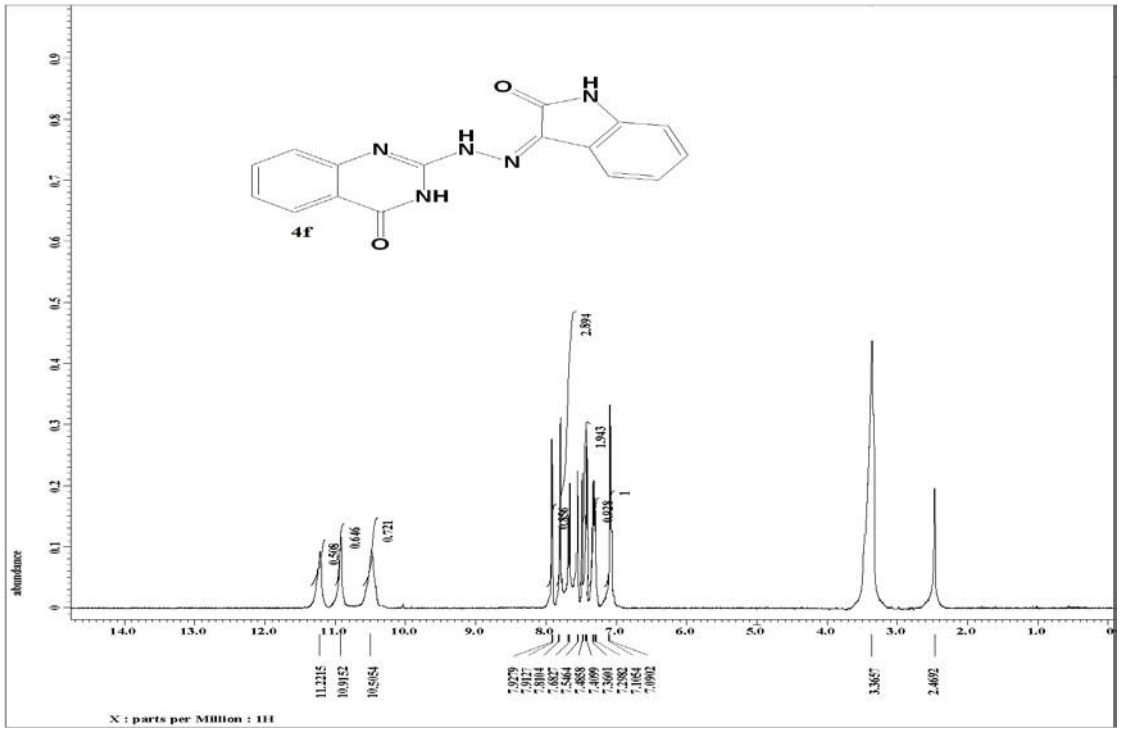


**Fig. S20** $^{1}$H NMR (500 MHz) in DMSO-$d_6$ of compound **4f**

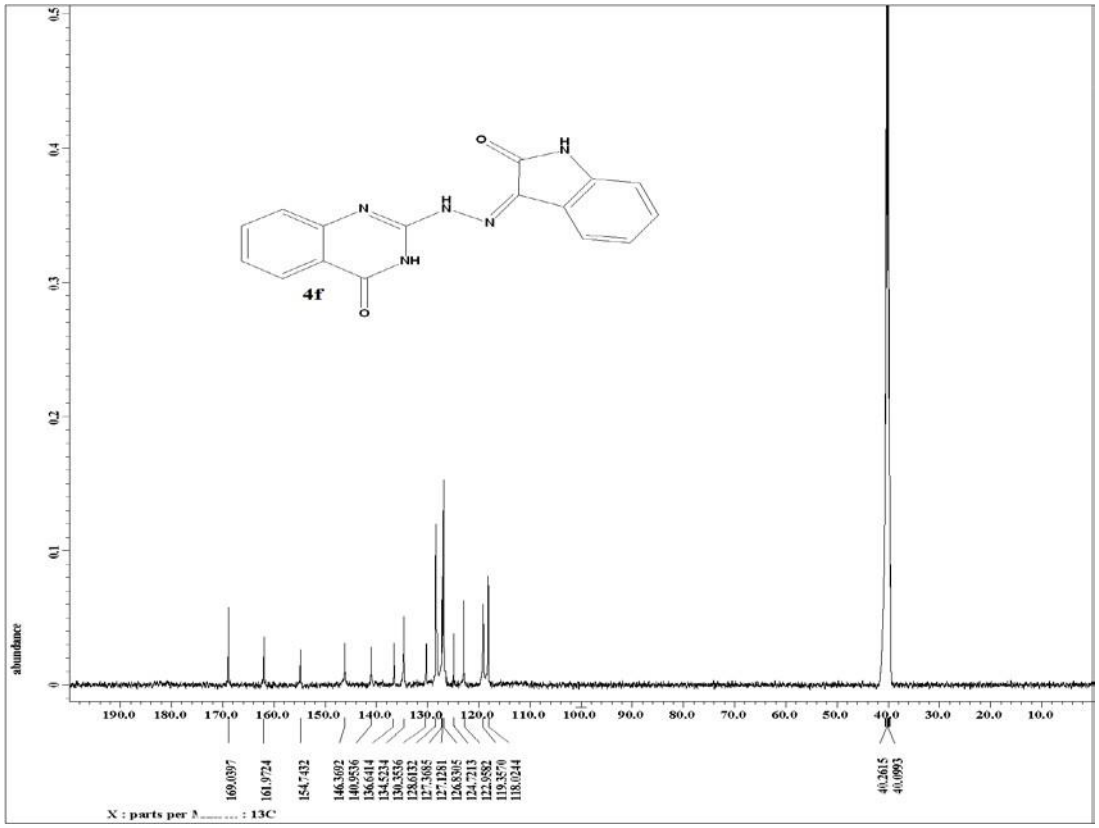


**Fig. S21** $^{13}$C NMR (125 MHz) in DMSO-$d_6$ of compound **4f.**

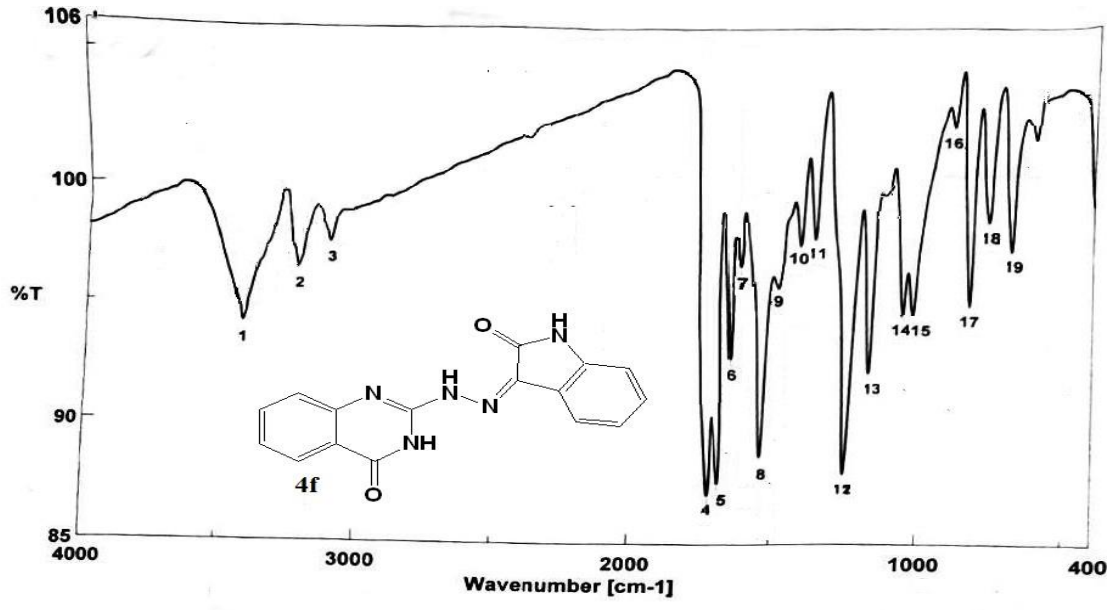


| No. | cm-1 | %T | No. | cm-1 | %T | No. | cm-1 | %T |
|---|---|---|---|---|---|---|---|---|
| 1 | 3432.67 | 94.1978 | 2 | 3201.57 | 96.2936 | 3 | 3062.77 | 97.6482 |
| 4 | 1699.48 | 87.1252 | 5 | 1671.48 | 87.5592 | 6 | 1633.92 | 92.2849 |
| 7 | 1596.41 | 96.1369 | 8 | 1533.41 | 88.6852 | 9 | 1475.43 | 95.6329 |
| 10 | 1371.14 | 97.3836 | 11 | 1325.03 | 97.1067 | 12 | 1252.03 | 88.1805 |
| 13 | 1177.33 | 91.8849 | 14 | 1061.62 | 94.2304 | 15 | 1027.87 | 94.2102 |
| 16 | 889.987 | 102.103 | 17 | 830.205 | 94.6369 | 18 | 765.601 | 98.1005 |
| 19 | 685.57 | 96.8823 | | | | | | |

**Fig. S22** I.R spectrum of compound **4f.**

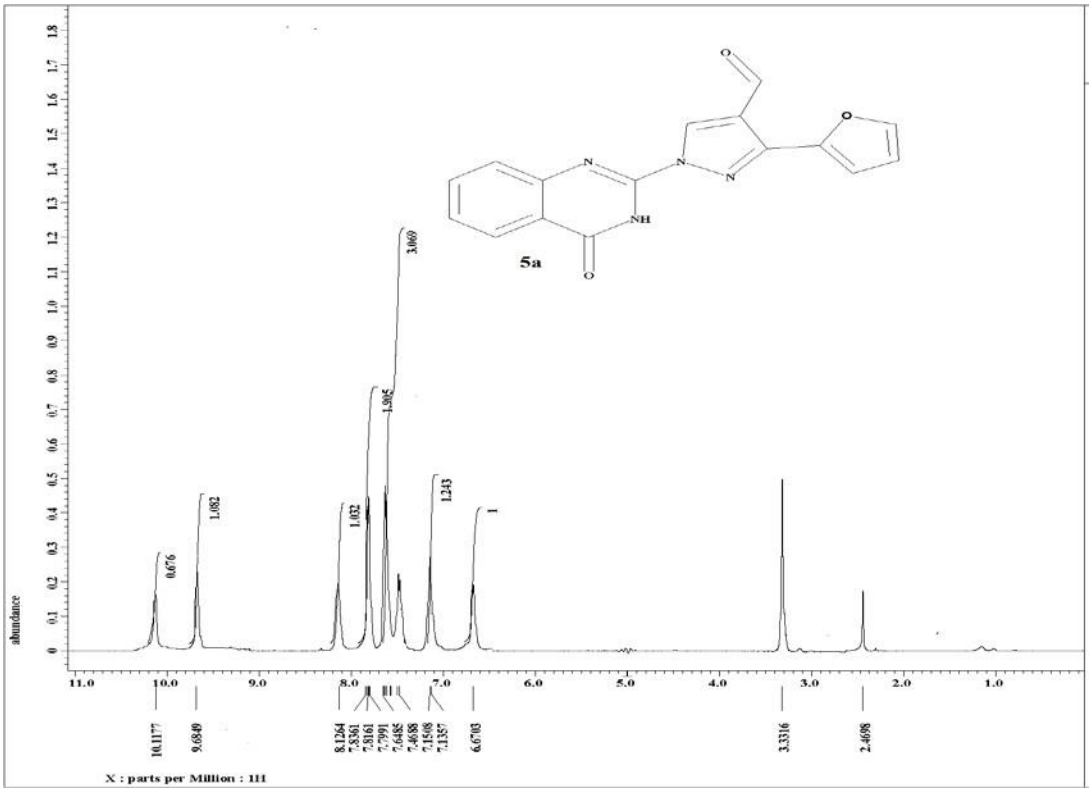


**Fig. S23** $^{1}$H NMR (500 MHz) in DMSO-$d_6$ of compound **5a**

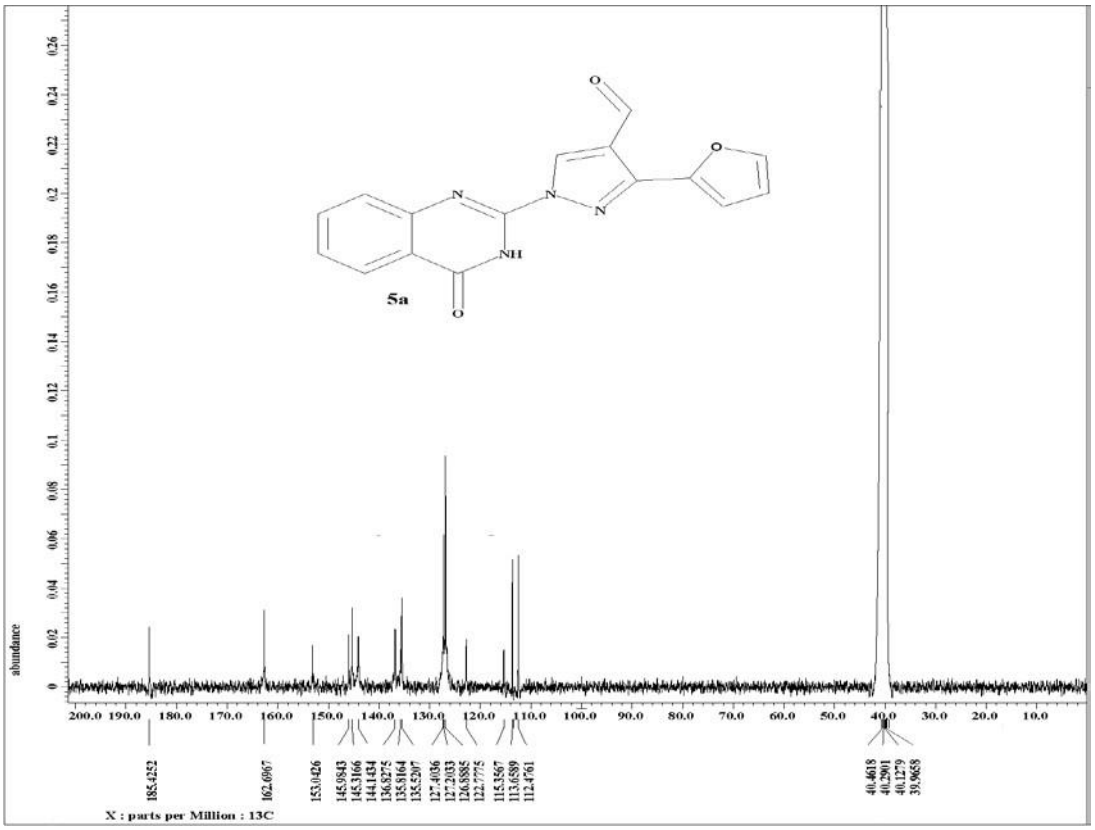


**Fig. S24** $^{13}$C NMR (125 MHz) in DMSO-$d_6$ of compound **5a.**

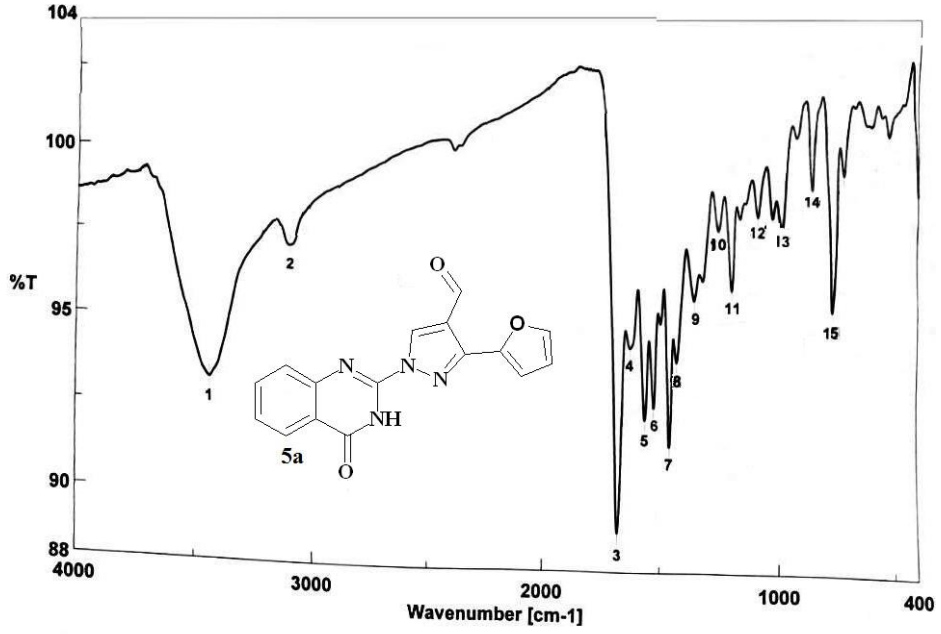


| No. | cm-1 | %T | No. | cm-1 | %T | No. | cm-1 | %T |
|---|---|---|---|---|---|---|---|---|
| 1 | 3434.6 | 93.2769 | 2 | 3089.9 | 97.2776 | 3 | 1680.66 | 89.1505 |
| 4 | 1628.59 | 94.587 | 5 | 1566.88 | 92.4524 | 6 | 1530.24 | 92.8075 |
| 7 | 1462.74 | 91.7072 | 8 | 1431.89 | 94.1935 | 9 | 1356.68 | 96.0196 |
| 10 | 1253.5 | 98.0704 | 11 | 1197.58 | 96.324 | 12 | 1081.87 | 98.5538 |
| 13 | 1018.23 | 98.5182 | 14 | 979.661 | 98.1909 | 15 | 851.418 | 99.3108 |

**Fig. S25** I.R spectrum of compound **5a.**

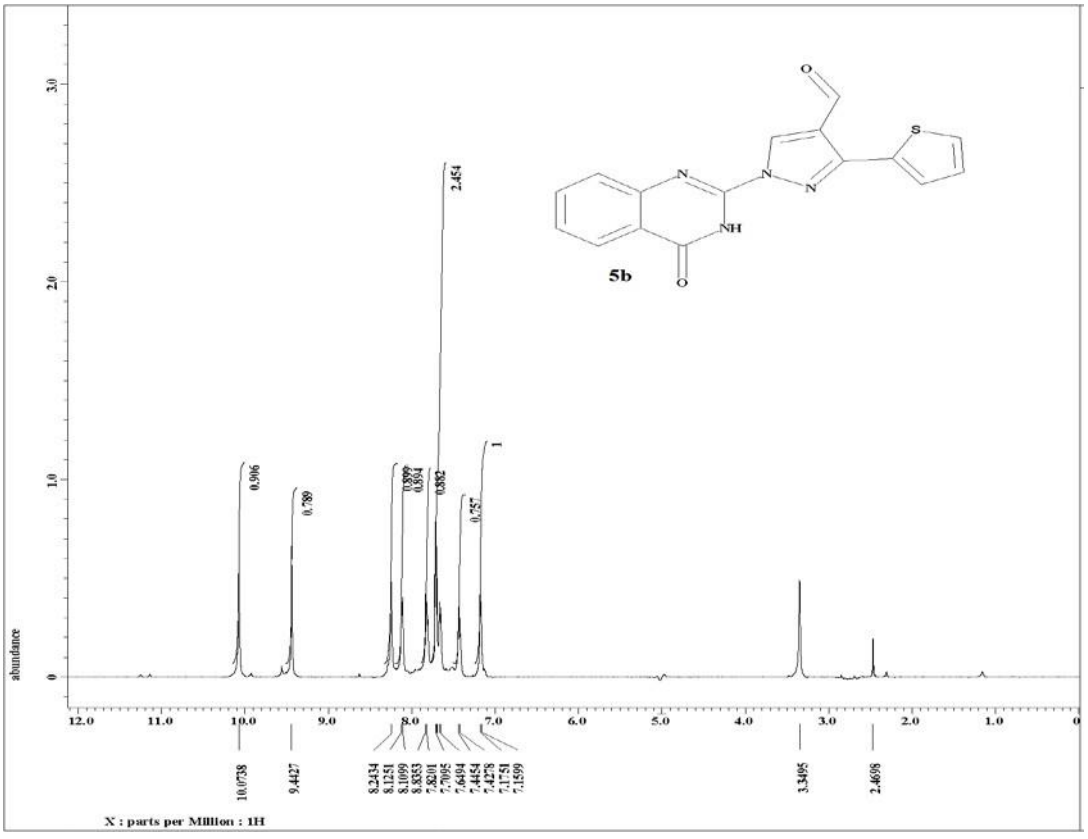


**Fig. S26** $^{1}$H NMR (500 MHz) in DMSO-$d_6$ of compound **5b.**

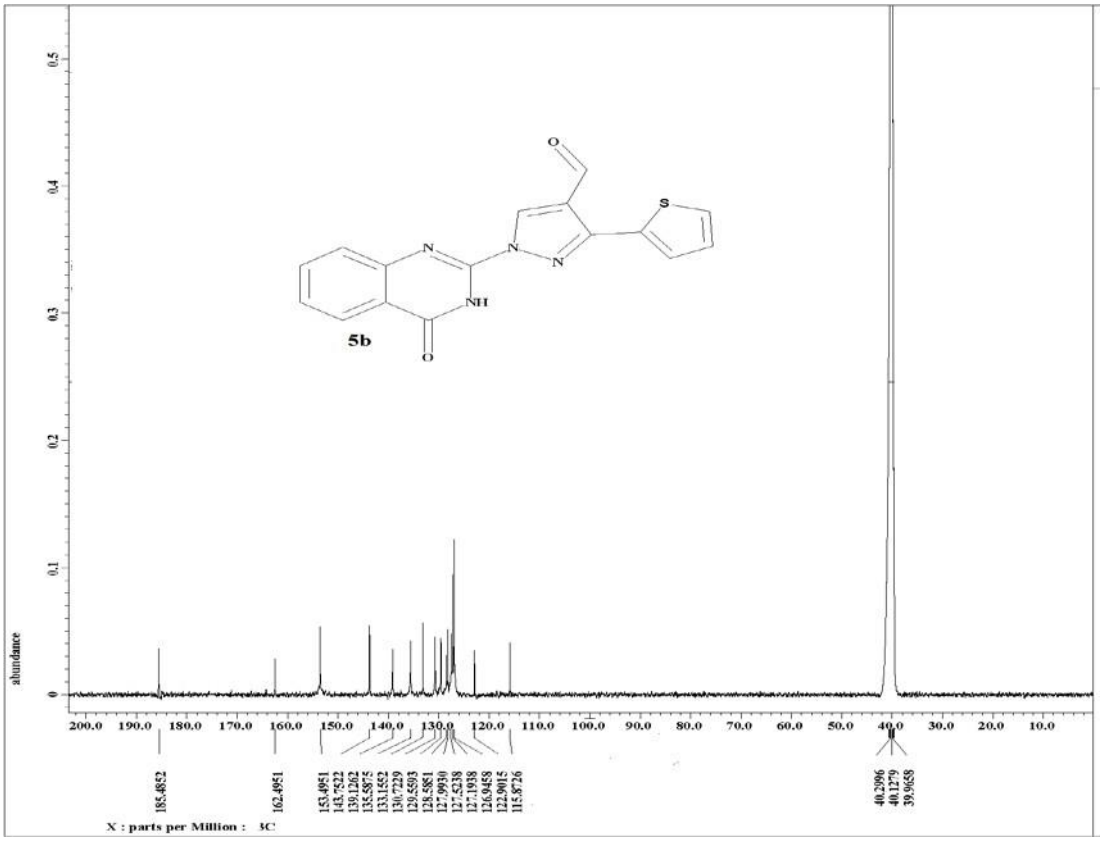


**Fig. S27** $^{13}$C NMR (125 MHz) in DMSO-$d_6$ of compound **5b.**

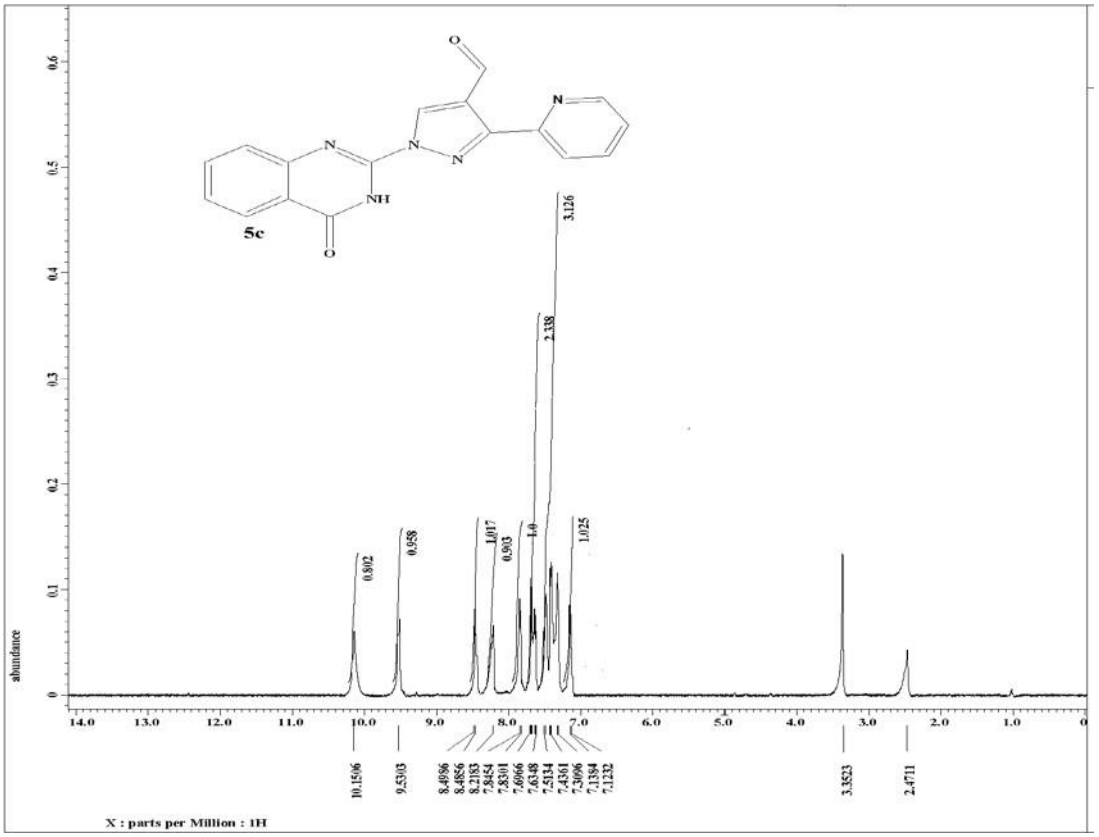

**Fig. S28** $^{1}$H NMR (500 MHz) in DMSO-$d_6$ of compound **5c.**

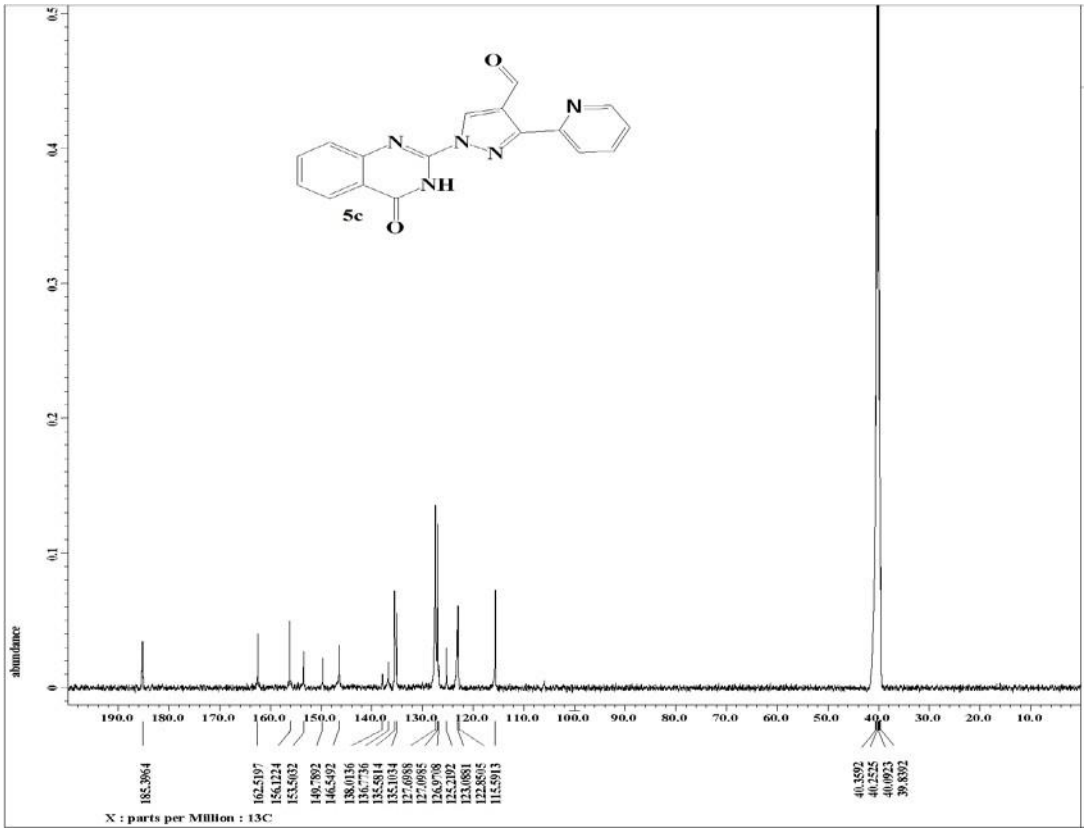


**Fig. S29** $^{13}$C NMR (125 MHz) in DMSO-$d_6$ of compound **5c.**

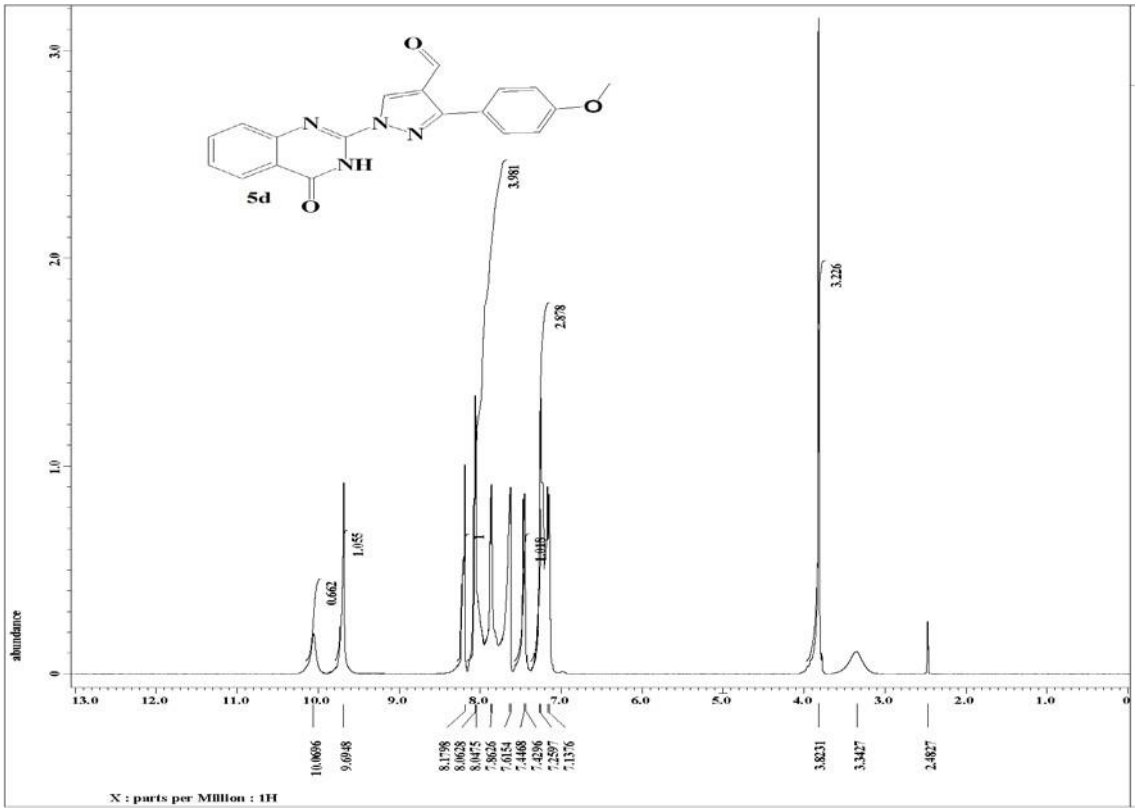


**Fig. S30** $^{1}$H NMR (500 MHz) in DMSO-$d_6$ of compound

**5d.**

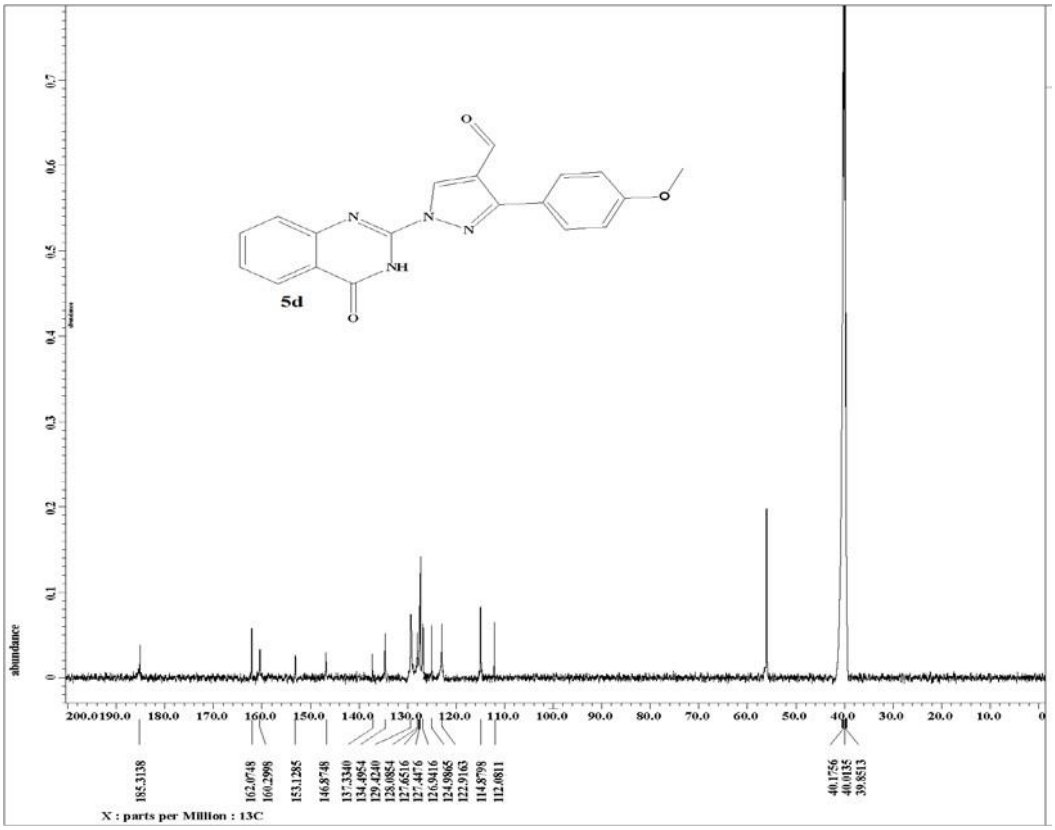


**Fig. S31** $^{13}$C NMR (125 MHz) in DMSO-$d_6$ of compound **5d**

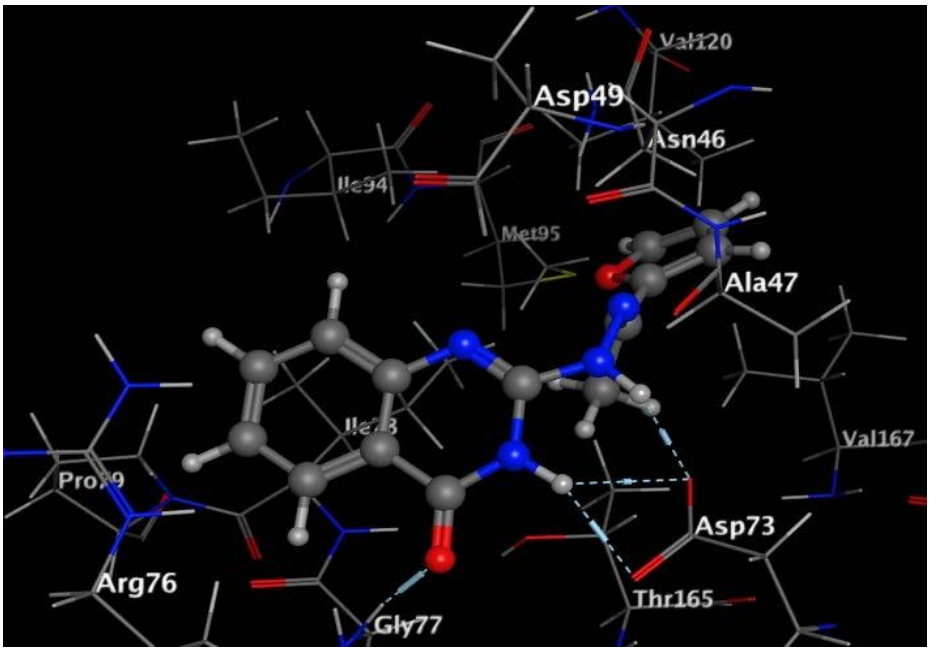
Asp49
Asn46
Met95
Ala47
Val167
Asp73
Arg76
Thr165
Gly77

A

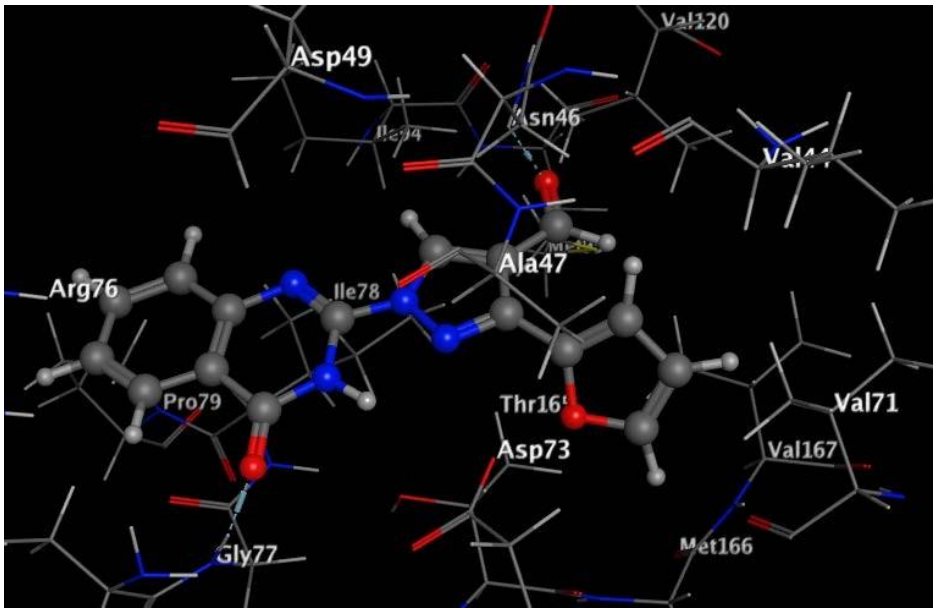
Asp49
Ala47
Arg76
Ile78
Pro79
Asp73
Val71
Val167
Gly77
Met166

B

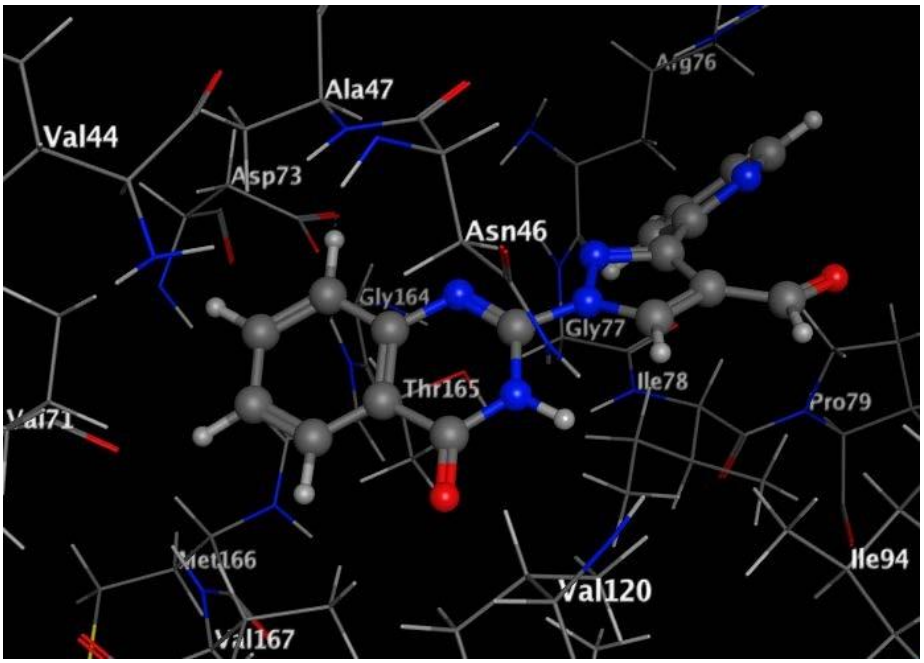


C

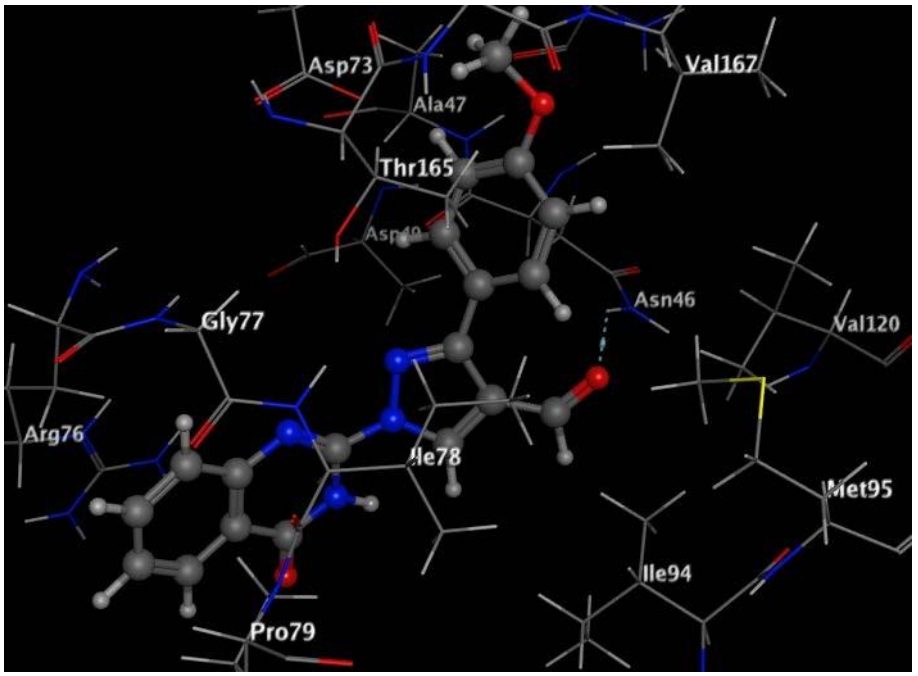


D

**Fig. S32.** A, B, C & D maps illustrate the 3D binding poses of the promising quinazolinone targets, **4a, 5a, 5c** and **5d** within the active site of *E. coli* DNA gyrase B (PDB code: 1AJ6).

**S33**

***Antimicrobial activity assay***

The biological potential of the newly prepared target structures was inspected toward the examined organisms and expressed as the diameter of the inhibition zones due to the agar plate diffusion technique. Also, the pathological strains (100µl) was outgrowing in 10 mL of fresh media till they reached a count of nearly $10^8$ cells/ml and

$10^5$ cells/mL for bacteria and fungi, respectively poured into 10cm diameter petri-

dishes. Also, (100µl) of each sample (200 µg) hold on filter paper disc (1.0 cm diameter). Prior to incubation, all prepared discs were deposited on to the surface of inoculated agar plates and kept at 4°C for two hours. The latter condition favors diffusion over microbial growth to clearly detect the inhibition zone. Whoever, incubation of plates was done for 24 h at 37 ˚C for bacteria, yeast and for 48 h at 30˚Cfor fungi activity. The plates were done in triplicate and the average inhibition zone diameters were recorded in mm and used as criterion for the microbial activity. Amoxicillin trihydrate was inspected as the antibacterial reference drug and clotrimazole was utilized as a standard antifungal drug. DMSO (solvent controls) was used for dissolving the examined compounds and illustrated no inhibition zone,

indicating that it has no effect on the growth of the tested biological strains.

**Minimum Inhibitory Concentration (MIC) Measurement**

The minimum Inhibitory Concentration activity of the compounds was then evaluated using broth dilution method. Whereas, two-fold serial dilution at the concentrations (0.25, 0.5, 1, 2, 4, 8, 16, 32, 64, 128 µg/ml) was used to investigate the Minimum Inhibitory Concentration (MIC) values (expressed in µg/mL) for the target compounds and the reference drugs. The tubes were then inoculated with the test organisms, grown in their suitable broth for 24 h

at 37 ˚C for bacteria, yeast and for 48 h at 30˚C for fungi activity ($1\times10^8$ CFU/mL for bacteria and 1 $x10^6$ CFU/mL of yeast and fungi), each 2 mL received 0.1 mL of the above inoculums Positive controls were prepared separately for either bacteria, yeast or fungi with respective organisms in the same culture media without the target compounds. After incubation, the tube with lowest concentration of extract that shows no growth was taken as the MIC value for the respective organism.

**S34**

*Escherichia coli* DNA Gyrase Supercoiling Inhibition Assay

The assay kits of *E. coli* DNA gyrase supercoiling was provided by TopoGEN, Inc. (Port Orange, FL) and the assays were performed according to established protocols obtained from the supplier. The new compounds and the standard inhibitor (novobiocin) were dissolved in DMSO and serially diluted at concentrations of 100, 10, 1 and 0.1 μM, and then assayed in reaction mixtures in three different replicate runs. The final reaction volume was 20 μL, which included 35 mM Tris pH 7, 2 mM DTT, 24 mM KCl, 4 mM $MgCl_2$, 1.8 mM spermidine, 0.1 mg/mL acetylated BSA, 6.5% (w/v) glycerol, 1 mM ATP, 0.1 mg/mL album and

0.2 mg pBR322 substrate. The reactions were initiated by addition of 2 U of *E.coli* DNA gyrase and 3 μL of inhibitor solution in 10% DMSO, and then were incubated with shaking for 30 minat 37 °C. All of the reactions were terminated by the addition of 10 mL of a 3X gel-loading buffer (final concentration: 6 mM EDTA, 1.2% SDS, 0.02% bromophenol blue, and 10% glycerolblue), after which 20 mL of this was loaded on a 1% agarose, TAE (0.01 M EDTA pH 8.3, 40 mMTris-acetate) gel that was then run at 60 V for 3 h. The gel was stained by (0.5 mg/L) ethidiumbromide in TAE for 30 min and then de-stained in water for 20 min. Fluorescent images were taken at a wavelength of 300 nm on a UV transilluminator imaging system. The fluorescence intensity of the supercoiled plasmid reaction product was quantitated using ImagQuant software. The results as IC50 values (concentration of the tested compound that leads to 50% inhibition of enzyme activity) for all samples were determined by nonlinear regression analysisin GraphPad Prism. The average $IC_{50}$ values (μM) of the triplicate experiments were calculated for the target compounds and the two reference antibiotics and then listed in Table 3.

**S35**

Molecular docking determination

The 2D structure of the newly synthesized quinazolinone derivatives **4a-c** and **5a-d** wasdrawn through chem. Draw. The protonated 3D was employed using standard bond lengths and angles, using Molecular Operating Environment (MOE-Dock) software version 2014.0901. Then, the geometry optimization and energy minimization were applied to get the Conf Search module in MOE, followed by saving of the moe file for upcoming docking process. The co-crystallized structure of *E. coli* DNA gyrase B kinase with its ligand novobiocin was downloaded (PDB code: 1AJ6) from protein data bank. All minimizations were performed using MOE until an RMSD gradient of 0.05 kcal·mol$^{-1}$Å$^{-1}$ with MMFF94x force field and the partial charges were automatically calculated. Preparation of the enzyme structure was done for molecular docking using Protonate 3D protocol with the default options in MOE. London dG scoring function and Triangle Matcher placement method were used in the docking protocol. At the first, validation of the docking process was established by docking of the native ligand, followed by docking of the derivatives **4a-c** and **5a-d** within the ATP-binding site after elimination of the co-crystallized ligand.